Summary of Theory Relating to Rydberg States of ^{87}Rb Atoms During Summer Project 2015-2016

Craig S. Chisholm*, Amita B. Deb and Niels Kjærgaard
chicr130@student.otago.ac.nz

Original version: January, 2016. This version: May, 2019

Contents

1 Radial Wavefunctions **2**
1.1 Quantum Defects 2
1.2 The Schrödinger Equation 2
1.3 The Numerov Algorithm 3

2 Matrix Elements, Lifetimes and Rabi Frequency **5**
2.1 Matrix Elements 5
2.2 Lifetimes 6
2.3 Rabi Frequency 8

3 The Blockade Shift **9**
3.1 Zero Field 9
3.2 Förster Resonances 9

References **13**

This document contains a summary of theoretical calculations relating to Rydberg atoms.

1 Radial Wavefunctions

To calculate the wave functions of electrons in Rydberg states, The Schrodinger equation was recast in atomic units and numerically integrated using the Numerov algorithm.[1]

1.1 Quantum Defects

The energy eigenvalues of the Rydberg states for Rb are given, in atomic units, by [1]

$$W = \frac{1}{2(n-\delta_{nlj})^2} \tag{1}$$

The parameter δ_{nlj} is called the quantum defect and is given by

$$\delta_{nlj} = \delta_0 + \frac{\delta_2}{(n-\delta_0)^2} + \frac{\delta_4}{(n-\delta_0)^4} + \cdots \tag{2}$$

where $\delta_0, \delta_2 \ldots$ depend on the quantum numbers n, l and j. The values of δ_0 and δ_2 are taken from [2] and [3]. For $n \geq 20$ terms involving powers of $\frac{1}{(n-\delta_0)}$ greater than 2 are ignored [2].

1.2 The Schrödinger Equation

The Schrödinger equation for a single electron in atomic units is [1]

$$[-\frac{1}{2\mu}\nabla^2 + V(r)]\psi(r,\theta,\phi) = W\psi(r,\theta\phi) \tag{3}$$

where μ is the reduced mass of the electron, r is the radial coordinate and $V(r)$ is a model potential. Since the Rb^+ ionic core is many thousands of times heavier than the single valence electron, the reduced mass, μ, is taken to be equal to the electron rest mass, m_e, which is equal to 1 in atomic units. The wavefunction may be seperated as $\psi(r,\theta,\phi) = R(r)Y_l^{ml}(\theta,\phi)$, where $Y_l^{ml}(\theta,\phi)$ is a spherical harmonic, because $V(r)$ has no angular dependence [1]. This gives the equation for the radial wave function

$$[-\frac{1}{2}(\frac{\mathrm{d}^2}{\mathrm{d}r^2} + \frac{2}{r}\frac{\mathrm{d}}{\mathrm{d}r}) + \frac{l(l+1)}{2r^2} + V(r)]R(r) = WR(r) \tag{4}$$

The potential is split in to two parts, $V(r) = V_c(r) + V_{SO}(r)$ [1]. The first term is a model core potential developed by Marinescu et al. [4] given by

$$V_c(r) = -\frac{Z_{nl}(r)}{r} - \frac{\alpha_c}{2r^4}(1 - \mathrm{e}^{-(r/r_c)^6}) \tag{5}$$

where

$$Z_{nl}(r) = 1 + (Z-1)\mathrm{e}^{-a_1 r} - r(a_3 + a_4 r)\mathrm{e}^{-a_2 r} \tag{6}$$

where Z is the nuclear charge of rubidium (37 in atomic units) and the parameters a_1 - a_4, r_c and α_c are determined empirically.

The second term describes the fine structure splitting caused by LS coupling and is given by [5]

$$V_{SO}(r) = \frac{\alpha^2}{2r^3}\mathbf{L}\cdot\mathbf{S} \tag{7}$$

where α is the fine structure constant and

$$\mathbf{L}\cdot\mathbf{S} = \frac{j(j+1) - l(l+1) - s(s+1)}{2} \tag{8}$$

where $s = \frac{1}{2}$ is the spin of an electron.

1.3 The Numerov Algorithm

The Schrödinger equation as given above does not permit analytic solutions to the radial wave equation so the task of finding the radial wavefunctions must be undertaken using numerical integration. The Numerov algorithm is particularly well suited to differential equations of the form [6]

$$\frac{\mathrm{d}^2Y}{\mathrm{d}x^2} = g(x)Y(x) \tag{9}$$

If the integration variable x increases with a constant stepsize h and we know $Y(x-h)$ and $Y(x)$ then we can calculate $Y(x+h)$ using

$$[1-T(x+h)]Y(x+h) + [1-T(x-h)]Y(x-h) = [2+10T(x)]Y(x) + O(h^6) \tag{10}$$

where $T(x) = \frac{h^2 g(x)}{12}$, if we ignore terms of order h^6. Note that the Numerov algorithm is symmetric in $x \pm h$ which is convenient since it is desirable to perform the integration backwards starting at $r_o = 2n(n+15)$ and ending in the vicinity of $r_i = \sqrt[3]{\alpha_c}$ in order to avoid the propagation of errors caused by the approximate model potential at short range [1].

In order to use the Numerov algorithm a change of variables must be applied in order to recast the radial wave equation in to the appropriate form. One way to do this is to define $x = \ln(r)$ and $Y(x) = R\sqrt{r}$ which recasts Eq. (4) in the form of Eq. (9) with [7]

$$g(x) = 2\mathrm{e}^{2x}\left(V - W\right) + \left(l + 1/2\right)^2. \tag{11}$$

Wavefunctions are normalised using

$$N^2 = \int_0^\infty r^2 R^2(r)\mathrm{d}r \tag{12}$$

which can be approximated as

$$N^2 \approx \sum_k r_k Y_k \Delta r_k \tag{13}$$

note that the variable x has evenly spaced step sizes but r does not.

Examples of radial wavefunctions and radial probability densities obtained by this method can be seen in figures 1 and 2 respectively.

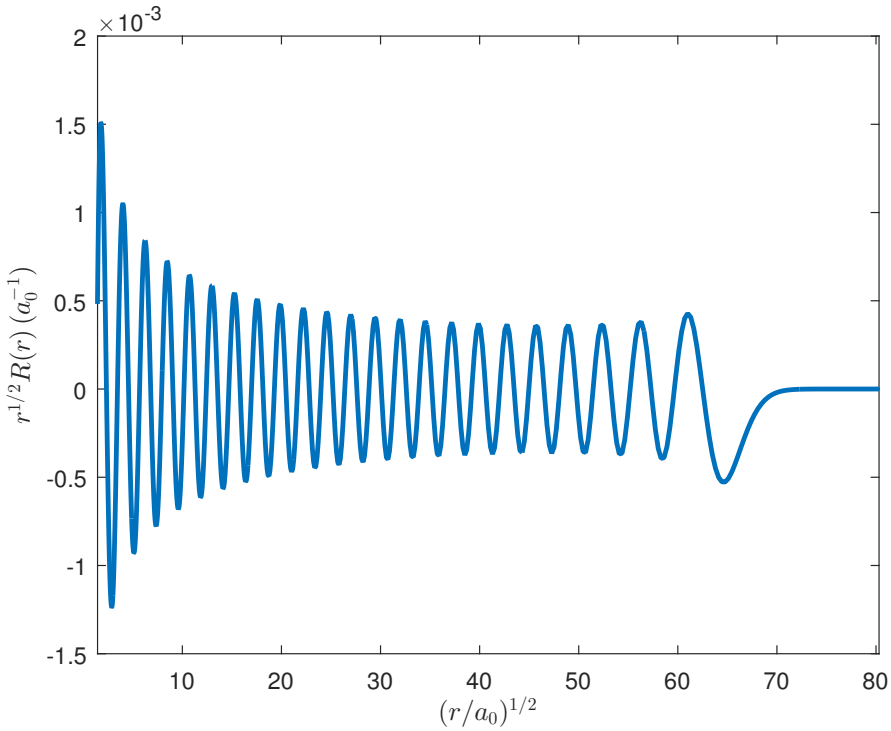

Figure 1: Radial wave function of $50^2\mathrm{S}_{\frac{1}{2}}$ state of Rb.

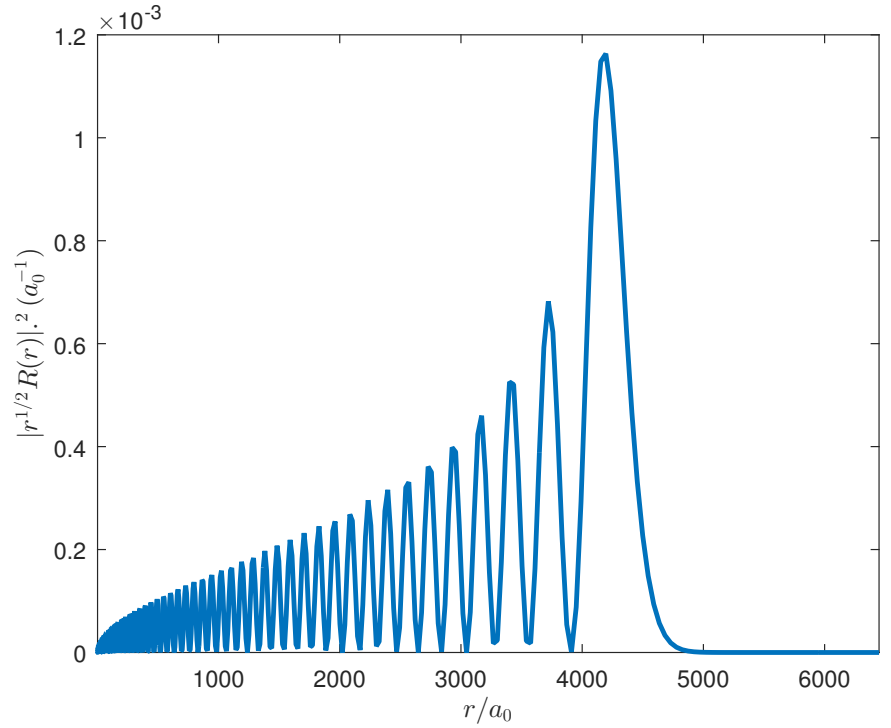

Figure 2: Radial probability density of $50^2\mathrm{S}_{\frac{1}{2}}$ state of Rb.

For purposes of calculations performed later in the document, wavefunctions corresponding to the ground states and the first several excited states (ignoring hyperfine structure) needed to be calculated. Data from NIST [8] was used to determine the exact energies of these states as the quantum defects would not give accurate energies in the $4 \leq n \leq 6$ regime. These energies were then used to compute

the wave functions using the model potential of [4]. To check the accuracy of the wave functions the $5^2S_{\frac{1}{2}}$ wavefunction was visually compared to a wavefunction determined by a self consistent field method [9], the two wavefunctions can be seen in figure 3 where it can be seen that good agreement is achieved.

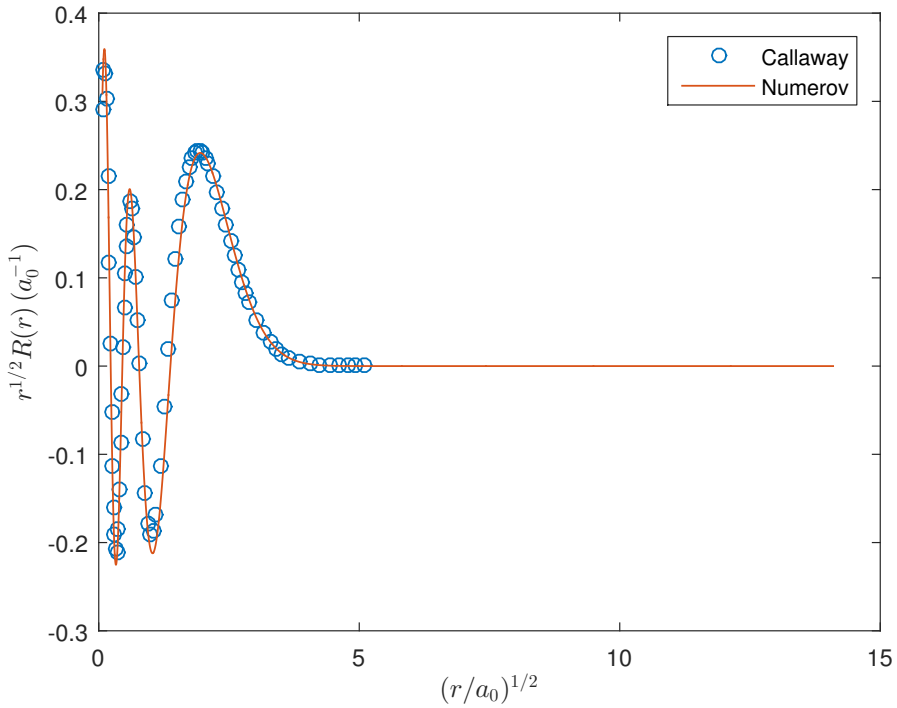

Figure 3: Groundstate wavefunction of Rubidium calculated by Numerov method with model potential [4] and self consistent field method [9].

2 Matrix Elements, Lifetimes and Rabi Frequency

2.1 Matrix Elements

In order to calculate many of the properties of Rydberg atoms, one must know the values of the matrix elements given by [1]

$$\langle nlj|er|n'l'j'\rangle = \int_{r_i}^{r_o} R_{n,l}(r) er R_{n',l'}(r) r^2 \mathrm{d}r \tag{14}$$

which is approximated as

$$\langle nlj|er|n'l'j'\rangle \approx \sum_k r_k^2 Y_k Y_k' \Delta r_k \tag{15}$$

Using these equations the value of $\langle 5,1,\frac{3}{2}|er|5,0,\frac{1}{2}\rangle$ was found to be $5.441ea_0$ which is inconsistent with the value of $4.221ea_0$ given by [10]. This discrepancy is attributed to errors due to the approximate potential at short range (where the low n wavefunctions are localised) [1]. Table 1 shows values of $\langle nlj|er|n'l'j'\rangle$ for Rydberg states obtained using the methods described above and by [11], the consistency in these values supports the attribution of the error in $\langle 5,1,\frac{3}{2}|er|5,0,\frac{1}{2}\rangle$ above.

Table 1: Calculated matrix elements of Rb Rydberg states from Durham group and this work.

Matrix element	Durham	This work
$\langle 46, 2, \frac{5}{2}\|er\|48, 1, \frac{3}{2}\rangle$	$1551ea_0$	$1551ea_0$
$\langle 46, 2, \frac{5}{2}\|er\|44, 3, \frac{7}{2}\rangle$	$1586ea_0$	$1586ea_0$
$\langle 46, 2, \frac{5}{2}\|er\|47, 1, \frac{3}{2}\rangle$	$2708ea_0$	$2708ea_0$
$\langle 46, 2, \frac{5}{2}\|er\|45, 3, \frac{7}{2}\rangle$	$2694ea_0$	$2694ea_0$
$\langle 50, 2, \frac{5}{2}\|er\|52, 1, \frac{3}{2}\rangle$	$1844ea_0$	$1843ea_0$
$\langle 50, 2, \frac{5}{2}\|er\|48, 3, \frac{7}{2}\rangle$	$1893ea_0$	$1892ea_0$
$\langle 35, 2, \frac{5}{2}\|er\|37, 1, \frac{3}{2}\rangle$	$877ea_0$	$877ea_0$
$\langle 35, 2, \frac{5}{2}\|er\|33, 3, \frac{7}{2}\rangle$	$882ea_0$	$882ea_0$

2.2 Lifetimes

Once, the matrix elements from the previous section are know, one can calculate the lifetimes of the Rydberg states. The lifetime of a state is determined by two factors: the radiative lifetime, τ_r, and the decay rate due to blackbody induced transitions, Γ_{BB}, the net lifetime is given by [6]

$$\frac{1}{\tau} = \frac{1}{\tau_r} + \Gamma_{BB} \tag{16}$$

where [10]

$$\frac{1}{\tau_r} = \frac{\omega_0^3}{3\pi\varepsilon_0\hbar c^3}\frac{2j+1}{2j'+1}|\langle nlj|er|n'l'j'\rangle|^2 \tag{17}$$

where ω_0 is the angular transition frequency from $|nlj\rangle \to |n'l'j'\rangle$ and an emperical model for the blackbody decay rate is given by [12]

$$\Gamma_{BB} = \frac{A}{n_{eff}^D}\frac{2.14\times 10^{10}}{\exp\left(315780B/n_{eff}^C T\right)-1}(s^{-1}) \tag{18}$$

where $n_{eff} = n - \delta_{nlj}$. The radiative lifetime is determined by allowed transitions. The allowed transitions follow the selections rules $\Delta l = \pm 1$ and $\Delta j = 0, \pm 1$ [15]. The lifetime due to each allwed decay pathway alone is calculated and the total radiative lifetime is found by summing these lifetimes reciprocally. Since the radiative lifetime for each decay path scales as ω_0^{-3}, only a small number of all possible decay paths are considered, specifically:

- $nS_{\frac{1}{2}} \to 6P_{\frac{3}{2}}, 6P_{\frac{1}{2}}, 5P_{\frac{3}{2}}, 5P_{\frac{1}{2}}$.
- $6P_{\frac{1}{2}} \to 6S_{\frac{1}{2}}, 5S_{\frac{1}{2}}, 4D_{\frac{3}{2}}$.
- $6P_{\frac{3}{2}} \to 6S_{\frac{1}{2}}, 5S_{\frac{1}{2}}, 4D_{\frac{5}{2}}, 4D_{\frac{3}{2}}$.
- $4D_{\frac{3}{2}} \to 6P_{\frac{3}{2}}, 6P_{\frac{1}{2}}, 5P_{\frac{3}{2}}, 5P_{\frac{1}{2}}$.
- $4D_{\frac{5}{2}} \to 6P_{\frac{3}{2}}, 5P_{\frac{3}{2}}$.

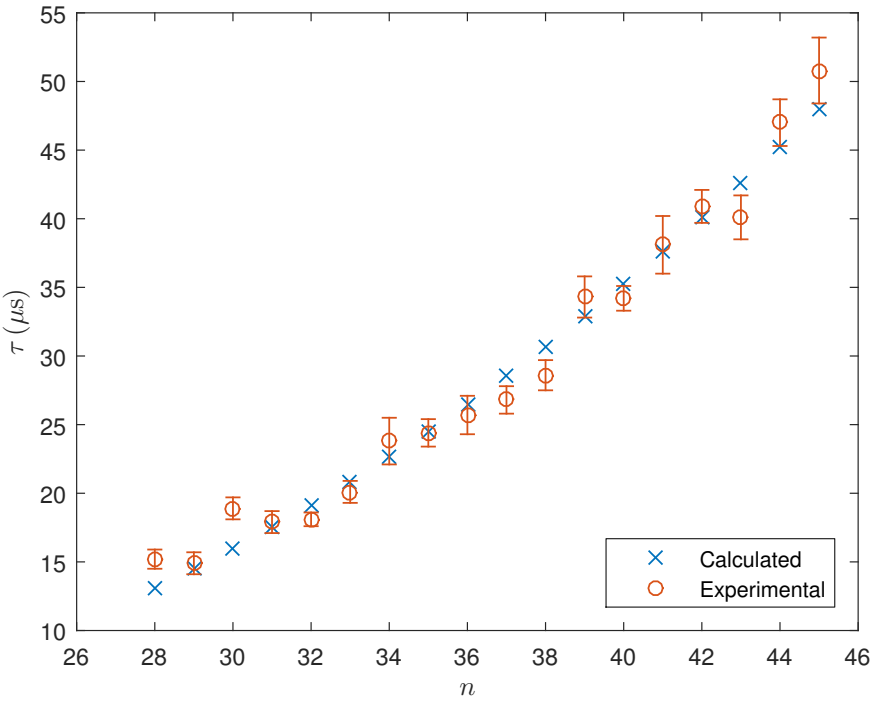

Figure 4: Calculated and experimental lifetimes of $nS_{\frac{1}{2}}$ states of Rb

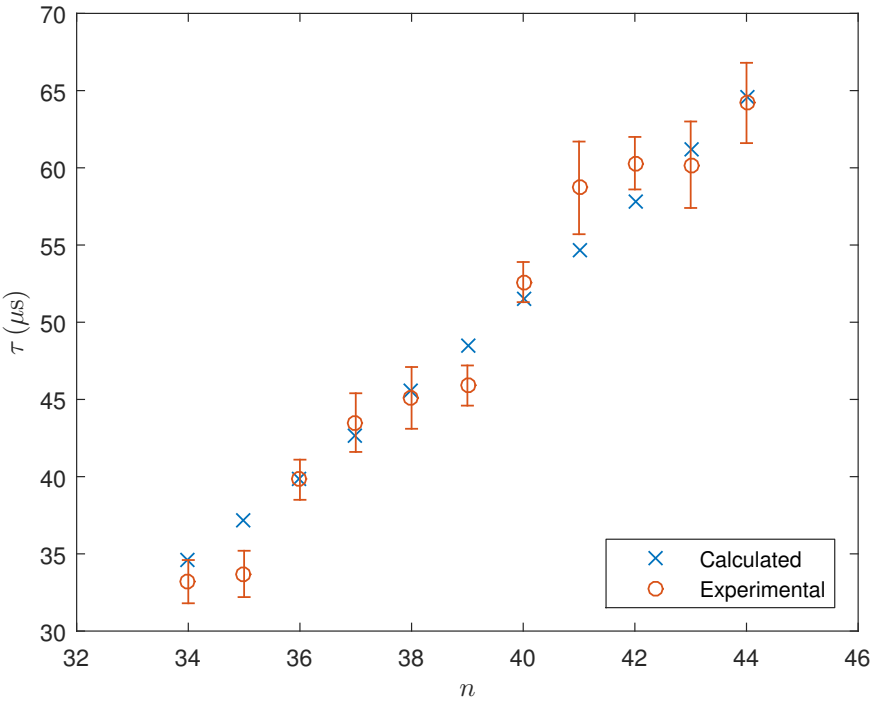

Figure 5: Calculated and experimental lifetimes of $nP_{\frac{3}{2}}$ states of Rb

Figures 4 - 6 give a visual comparisson of values calculated using this method and the experimental values of [13]. As can be seen from figures 4 - 6, there is good agreement between calculation and experiment for $nS_{\frac{1}{2}}$ and $nP_{\frac{3}{2}}$ states but the calculated $nD_{\frac{5}{2}}$ states appear to be consistently underestimated. Howevere, more recent work [14] has measured the life time of the $38D_{\frac{5}{2}}$ state to be 13(4) μs, which is in better agreement with the calculated value of 16.2 μs in this work.

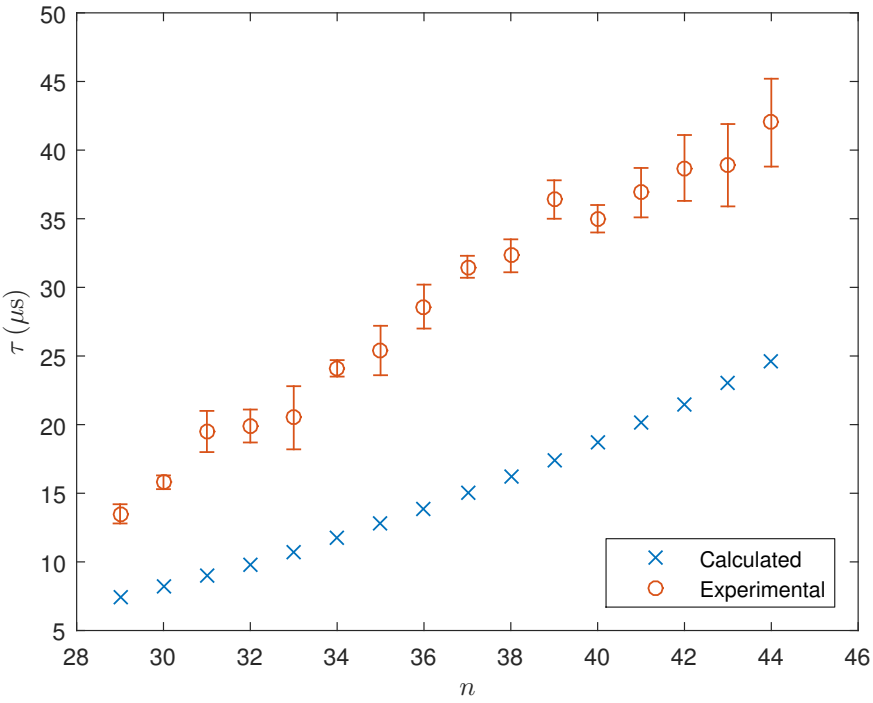

Figure 6: Calculated and experimental lifetimes of $nD_{\frac{5}{2}}$ states of Rb

2.3 Rabi Frequency

Once the radial matrix elements are known, they may beused to calculate the necessary laser power to achieve a particular Rabi frequency for a given transition and beam waist. The Rabi frequency is related to the intensity of laser light and the dipole matrix element of the transtion by [16]

$$\Omega = \sqrt{\frac{2I}{\varepsilon_0 \hbar^2 c}} \langle n'l'j'm'_j | er_q | nljm_j \rangle \tag{19}$$

Where q represents the polarisation of light and the relationship $m'_j = m_j - q$ is satisfied. The matrix element including the fine structure splitting is given by [1]

$$\begin{aligned} \langle nljm_j | er_q | n'l'j'm'_j \rangle = (-1)^{j-m_j+s+j'+1} \sqrt{(2j+1)(2j'+1)(2l+1)(2l'+1)} \\ \times \begin{Bmatrix} j & 1 & j' \\ l' & s & l \end{Bmatrix} \begin{pmatrix} j & 1 & j' \\ -m_j & q & m_j \end{pmatrix} \begin{pmatrix} l & 1 & l' \\ 0 & 0 & 0 \end{pmatrix} \langle nlj | er | n'l'j' \rangle. \end{aligned} \tag{20}$$

The fine structure basis gives good quantum numbers for the Rydberg atoms but the transition to the Rydberg state is $5S_{\frac{1}{2}} \rightarrow 5P_{\frac{3}{2}} \rightarrow |r\rangle$ and the good quantum numbers are F and m_F so we assume the first transition to the hyperfine sublevel $|5, 1, \frac{3}{2}, F = 2, m_F = 2\rangle$ and decompose in the fine structure basis using Clebsch-Gordan coefficients. Rearranging Eq. (19) for intensity then gives

$$I = \frac{1}{\sum_{j,m_j} \langle n'l'j'm'_j | C^{F=2,m_F=2}_{j,m_j} r_q | 5, 1, j, m_j \rangle} \frac{\varepsilon_0 \hbar^2 c}{2e^2} \tag{21}$$

The necessary power for a given beam waist, w_0, can then be calculated using [17]

$$P = \frac{\pi}{2} I w_0^2 \tag{22}$$

Some example calculations are given in table 2.

Table 2: Calculated power for arbitrary Rabi frequency $\Omega = 1MHz$ assuming polarisation $q = +1$ with nominal beam waist $w_0 = 30\mu m$.

State	Power (mW)
$50S_{\frac{1}{2}}$	2.042
$60S_{\frac{1}{2}}$	3.628
$70S_{\frac{1}{2}}$	5.812
$50D_{\frac{5}{2}}$	1.709
$60D_{\frac{5}{2}}$	3.048
$70D_{\frac{5}{2}}$	5.064

3 The Blockade Shift

3.1 Zero Field

Since the valence electrons of Rydberg atoms are in states with very large principle quantum number n, they are very delocalised from the ionic core. This gives Rydberg atoms their characteristic large sizes and polarisabilities leading to strong dipolar interactions, also known as the blockade shift. Where the dipole operator is given by (in atomic units) [18]

$$\begin{aligned} V_{dd} = & \frac{p_{1+}p_{2-} + p_{1-}p_{2+} + p_{10}p_{20}(1 - 3\cos^2\theta)}{R^3} \\ & - \frac{\frac{3}{2}\sin^2\theta(p_{1+}p_{2+} + p_{1+}p_{2-} + p_{1-}p_{2+} + p_{1-}p_{2-})}{R^3} \\ & - \frac{\frac{3}{\sqrt{2}}\sin\theta\cos\theta(p_{1+}p_{20} + p_{1-}p_{20} + p_{10}p_{2+} + p_{10}p_{2-})}{R^3} \end{aligned} \tag{23}$$

where $p_q = er_q$ and the subscripts 1 and 2 indicate atom label. Second order perturbation theory gives an energy shift of

$$\Delta W^{(2)} = - \sum_{\substack{n',l',j',m'_j \\ n'',l'',j''m''_j}} \frac{|\langle n'', l'', j'', m''_j| \otimes \langle n', l', j', m'_j|V_{dd}|n, l, j, m_j\rangle \otimes |n, l, j, m_j\rangle|^2}{\Delta}. \tag{24}$$

Where $\Delta = W_{|n'',l'',j''.m''_j\rangle} + W_{|n',l',j',m'_j\rangle} - 2W_{|n,l,j,m_j\rangle}$ is the infinite-separation energy defect. We consider all states with $|\Delta| < 100GHz$ and $|n - n''|, |n - n'| \leq 4$. One would not expect exact answers using perturbation theory but comparisson with [19] indicates a good order of magnitude estimate.

An example of the blockade shift for $50S_{\frac{1}{2}}$ is given in figure 7. Values of $|C_6|$ obtained with θ chosen to maximise the shift in all cases, are plotted against n for $nS_{\frac{1}{2}}$, $nD_{\frac{3}{2}}$ and $nD_{\frac{5}{2}}$ states are shown in figures 8 - 10 respectively.

3.2 Förster Resonances

From figure 8 it is clear that there is a very rapid increase in the magnitude of the blockade shift as n is increased, although these values (particularly those at

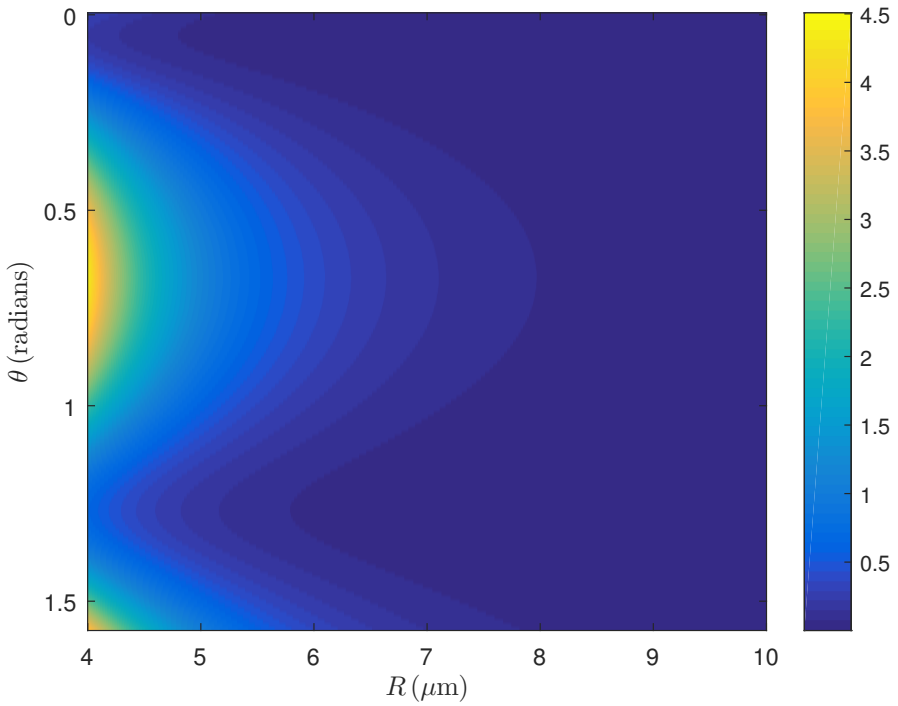

Figure 7: Calculated blockade shift for $50S_{\frac{1}{2}}$ state.

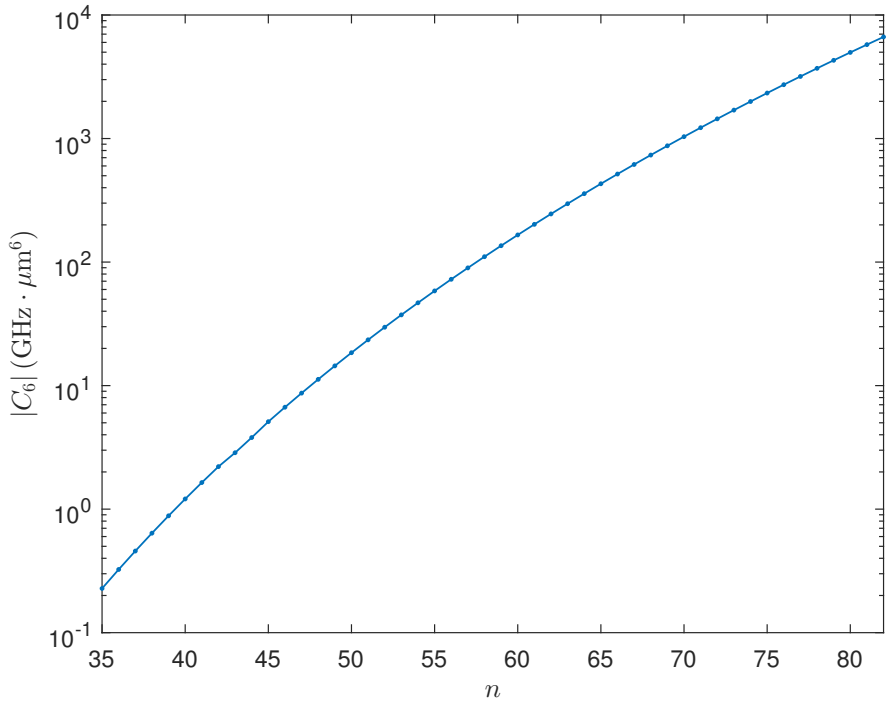

Figure 8: Calculated $|C_6|$ against n for $nS_{\frac{1}{2}}$ state.

high n) must be taken with a grain of salt as results from perturbation theory tend to break down as the perturbation becomes larger [20]. Figures 9 and 10 are more interesting showing points where the magnitude of the blockade shift is much higher than the trend would predict and where, while not apparent from plots of $|C_6|$, the blockade shift changes sign. These are due to Förster resonances or near Förster resonances where the infinite separation energy defect is very small or zero for an

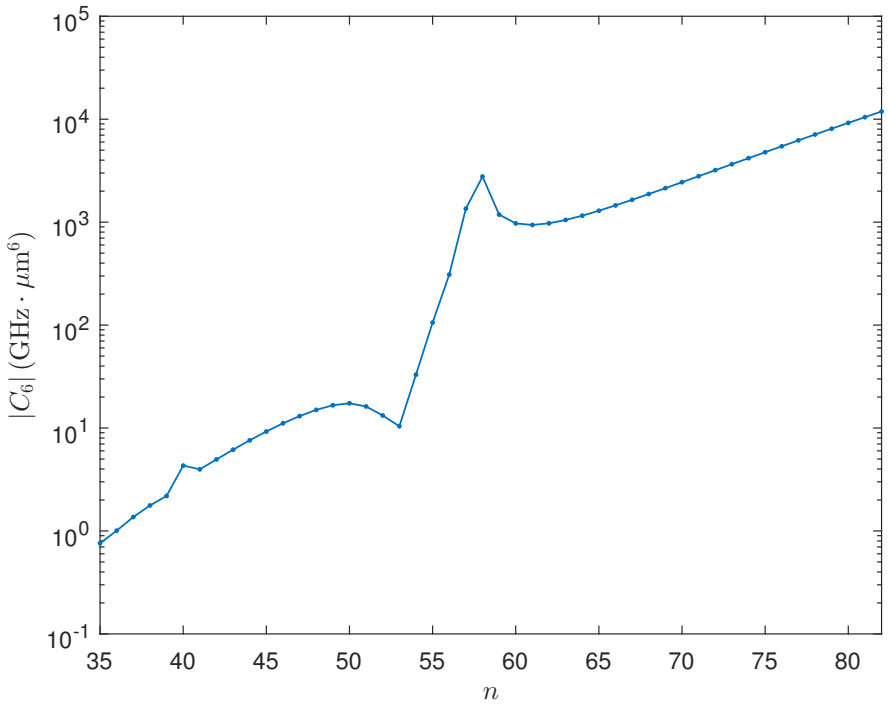

Figure 9: Calculated $|C_6|$ against n for $nD_{\frac{3}{2}}$ state.

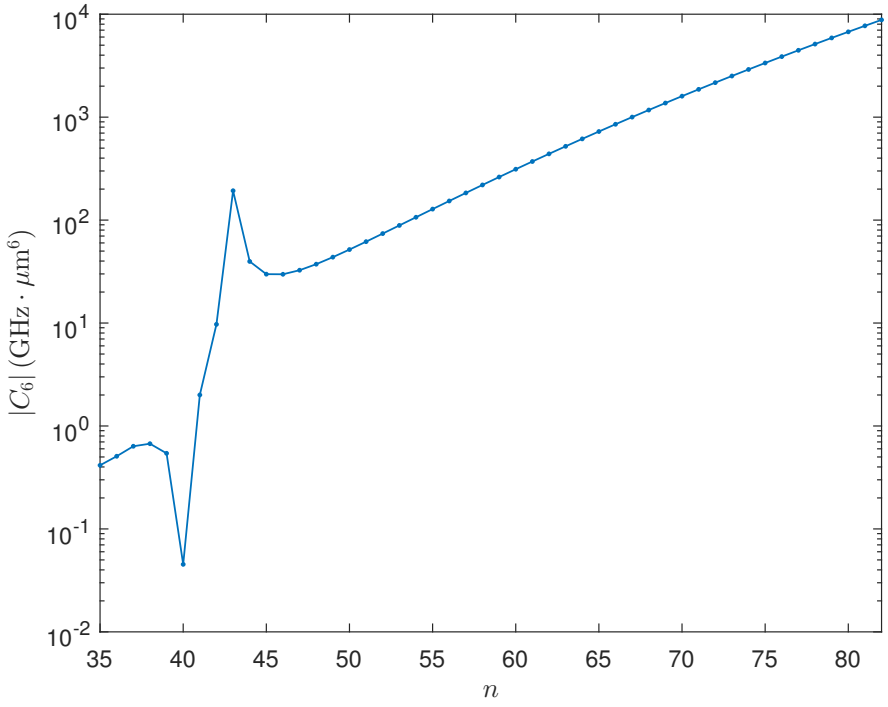

Figure 10: Calculated $|C_6|$ against n for $nD_{\frac{5}{2}}$ state.

exact resonance [21]. The resonance at $n = 58$ for the $nD_{\frac{3}{2}}$ states is due to the interaction chanel [18]

$$2 \times |58D_{\frac{3}{2}}\rangle \rightarrow |60P_{\frac{1}{2}}\rangle \otimes |56F_{\frac{5}{2}}\rangle$$

while the resonance at $n = 43$ for the $|nD_{\frac{5}{2}}\rangle$ states is due to the interaction chanel [18]

$$2 \times |43D_{\frac{5}{2}}\rangle \rightarrow |45P_{\frac{3}{2}}\rangle \otimes |41F_{\frac{7}{2}}\rangle.$$

The $nD_{\frac{3}{2}}$ series also has a smaller near resonance around $n \approx 40$. Near resonances may be tuned to exact resonances using the Stark effect [19].

References

[1] J. D. Pritchard, *Cooperative Optical Non-Linearity in a Blockaded Rydberg Ensemble*, Springer-Verlag, Berlin Heidelberg, 2012.

[2] W. Li, I, Mourachko, M. W. Noel, T. F. Gallagher, *Millimeter-Wave spectroscopy of cold Rb Rydberg atoms in a magneto-optical trap: quantum defects of the ns, np and nd series*. Phys. Rev. A **67**, 052502 (2003).

[3] J. Han, Y. Jamil, D. V. L. Norum, P. J. Tanner, T. F. Gallagher, *Rb nf quantum defects from millimeter-wave spectroscopy of cold ^{85}Rb atoms*. Phys. Rev. A. **74**(5), 054502 (2006).

[4] M. Marinescu, H. R. Sadeghpour, A. Dalgarno, *Dispersion coefficients of alkali metal dimers*. Phys. Rev. A **49**(2), 982 (1994).

[5] C. E. Theodosiou, *Lifetimes of alkali-metal-atom Rydberg states*. Phys. Rev. A **30**(6), 2881-2909 (1984).

[6] T. F. Gallagher, *Rydberg Atoms*. Cambridge University Press (2005).

[7] M. L. Zimmerman, M. G. Littman, M. M. Kash, D. Kleppner, *Stark structure of the Rydberg states of alkali-metal atoms*. Phys. Rev. A **20**(6), 2251 (1979).

[8] I. Johansson, Ark. Fys. **20**, 135 (1961).

[9] J. Callaway, D. F. Morgan, Jr., *Cohesive Energy and Wave Functions for Rubidium*. Phys. Rev **112**, 2 (1958).

[10] D. A. Steck, *Rubidium 87 D Line Data* http://steck.us/alkalidata (2003).

[11] J. D. Pritchard, *Calculation of Rydberg atom wavefunctions and Stark maps* massey.dur.ac.uk/jdp/talks_and_posters.html

[12] I. I. Beterov, I. I. Ryabstev, D. B. Tretyakov, V. M Entin, *Quasiclassical calculations of blackbody-radiation-induced depolution rates and effective lifetimes of Rydberg nS, nP, and nD alkali-metal atoms with $n \leq 80$*. Phys. Rev. A **79**, 052504 (2009).

[13] D. B. Branden, T. Juhasz, T Mahlokozera, C. Vesa, R. O. Wilson, M. Zheng, A. Kortyna, D. A. Tate, *Radiative lifetime measurements of rubidium Rydberg states*. J. Phys. B: At. Mol. Phys. **43**, 1 (2009).

[14] M. Mack, J. Grimmel, F. Karlewski, L. Sárkány, H. Hattermann, J Fortágh. *All-optical measurement of Rydberg-state lifetimes* Phys. Rev. A **92**, 012517 (2015)/

[15] M. Weissbluth, *Atoms and Molecules*. Academic Press, New York, 1978.

[16] H. J. Metcalf, *Laser Cooling and Trapping*. Springer-Verlag, New York (1999).

[17] E. Hecht, *Optics* 4^{th} ed. Addison-Wesley (2002).

[18] A. Reinhard, T. Cubel Liebisch, B. Knuffman, G. Raithel, *Level shifts of rubidium Rydberg states due to binary interactions*. Phys, Rev a **75**, 032712 (2007).

[19] L. Béguin, A. Vernier, R. Chicireanu, T. Lahaye, A. Browaeys, *Direct Measurement of the van der Waals Interaction between Two Rydberg Atoms*. Phys. Rev. Lett **110**, 263201 (2013).

[20] D. H. McIntyre, C. A. Manogue, J. Tate, *Quantum Mechanics* 1^{st} ed. Pearson Education, Edinburgh (2014).

[21] D. Comparat, P. Pillet, *Dipole blockade in a cold atomic sample* J. Opt. Soc. Am. B **27**(6), 125243 (2010).